

Cite as: R. P. Dias *et al.*, *Science*  
10.1126/science.aal1579 (2017).

# Observation of the Wigner-Huntington transition to metallic hydrogen

Ranga P. Dias and Isaac F. Silvera\*

Lyman Laboratory of Physics, Harvard University, Cambridge, MA 02138, USA.

\*Corresponding author. Email: silvera@physics.harvard.edu

**Producing metallic hydrogen has been a great challenge to condensed matter physics. Metallic hydrogen may be a room temperature superconductor and metastable when the pressure is released and could have an important impact on energy and rocketry. We have studied solid molecular hydrogen under pressure at low temperatures. At a pressure of 495 GPa hydrogen becomes metallic with reflectivity as high as 0.91. We fit the reflectance using a Drude free electron model to determine the plasma frequency of  $32.5 \pm 2.1$  eV at  $T = 5.5$  K, with a corresponding electron carrier density of  $7.7 \pm 1.1 \times 10^{23}$  particles/cm<sup>3</sup>, consistent with theoretical estimates of the atomic density. The properties are those of an atomic metal. We have produced the Wigner-Huntington dissociative transition to atomic metallic hydrogen in the laboratory.**

Several key problems in physics involving hydrogen include production of the metallic phase, high temperature superconductivity, and controlled nuclear fusion (1). The transition to solid metallic hydrogen (SMH) was envisioned by Wigner and Huntington (WH) over 80 years ago (2). They predicted a first-order dissociative transition to an atomic lattice through compression of solid molecular hydrogen to a sufficiently high density. Solid atomic hydrogen would be a metal with one electron per atom with a half filled conduction band. Although WH's density for the transition was approximately correct, their predicted pressure of 25 GPa (100 GPa = 1 megabar) was way off as they incorrectly used the zero-pressure compressibility for all pressures. Wigner and Huntington predicted a simple phase diagram. Enormous experimental and theoretical developments dramatically reshaped the phase diagram of hydrogen (Fig. 1) over the past decades. Modern quantum Monte-Carlo methods and density functional theory predict pressures of ~400 to 500 GPa for the transition (3–5), with an atomic lattice being in the  $I_{41}/amd$  space group (5, 6). Metallic hydrogen (MH) may be a high temperature superconductor, predicted by Ashcroft (7), with critical temperatures possibly higher than room temperature (8, 9). Moreover, other predictions suggest SMH is metastable at room temperature when the pressure is released (10). The combination of these expected properties make SMH important for solving energy problems and can potentially revolutionize rocketry as a powerful propellant (11).

The pathways to metallic hydrogen require either increasing pressure at low temperature (Fig. 1, Pathway I) or increasing temperature to cross the plasma phase transition (12–17) (Fig. 1, Pathway II). Pathway I transitions through a number of phases not envisioned in the simple phase dia-

gram predicted by WH. The low-pressure properties of solid molecular hydrogen are fascinating and many aspects such as the importance of ortho-para concentrations, and solid-solid phase transitions characterized by orientational order have been reviewed elsewhere (3, 18). In the low-pressure low-temperature phase I, molecules are in spherically symmetric quantum states and form a hexagonal-close-packed structure. Phase II, III, and IV are phases with structural changes and orientational order of the molecules (19–23). A new phase in hydrogen observed at liquid helium temperatures believed to precede the metallic phase was called H<sub>2</sub>-PRE (24) (also named VI at higher temperatures (25)).

We carried out a rigorous strategy to achieve the higher pressures needed to transform to SMH in a diamond anvil cell (DAC). Diamond failure is the principal limitation for achieving the required pressures to observe SMH. We believe that one point of failure of diamonds arises from microscopic surface defects created in the polishing process. We used type IIa conic synthetic diamonds (supplied by Almax-Easylab) with ~30 micron diameter culet flats. We etched off about 5 microns from the diamond culets using reactive ion etching to remove surface defects (figs. S7 and S8) (26). We vacuum annealed the diamonds at high temperature to remove residual stresses. A second point of failure is diamond embrittlement from hydrogen diffusion. Hydrogen can disperse into the confining gasket or the diamonds (at high pressure or temperature). As an activated process, diffusion is suppressed at low temperatures. We maintained the sample at liquid nitrogen or liquid helium temperatures during the experimental runs. Alumina is also known to act as a diffusion barrier against hydrogen. We coated the diamonds along with the mounted rhenium gasket with a 50 nm thick layer of amorphous alumina by the

process of atomic layer deposition. We have found through our extensive experience with alumina coatings at high pressures that it does not affect or contaminate the sample, even at temperatures as high as  $\sim 2000$  K (12). Finally, focused laser beams, even at low laser power (10 mW) on samples at high pressures in DACs, can also lead to failure of the highly stressed diamonds. Laser light in the blue spectral region appears to be particularly hazardous as it potentially induces the growth of defects (27). Thermal shock to the stressed culet region from inadvertent laser heating is another risk. Moreover, a sufficiently intense laser beam, even at infrared (IR) wavelengths, can graphitize the surface of diamond. Thus, we studied the sample mainly with very low power incoherent IR radiation from a thermal source, and minimized illumination of the sample with lasers when the sample was at very high pressures.

We cryogenically loaded the sample chamber at 15 K, which included a ruby grain for pressure determination. We initially determined a pressure of  $\sim 88$  GPa by ruby fluorescence (26). Determining the pressure in the megabar regime is more challenging (26). We measured the IR vibron absorption peaks of hydrogen at higher pressures ( $>135$  GPa) with a Fourier transform infrared spectrometer with a thermal IR source, using the known pressure dependence of the IR vibron peaks for pressure determination (26). We did this to a pressure of  $\sim 335$  GPa, while the sample was still transparent (Fig. 2A). The shift of the laser excited Raman active phonon of the diamond in the highly stressed culet region is currently the method used for determining pressure at extreme high pressures. For fear of diamond failure due to laser illumination and possible heating of the black sample, we only measured the Raman active phonon at the very highest pressure of the experiment (495 GPa) after the sample transformed to metallic hydrogen and reflectance measurements had been made. We equip our DACs with strain gauges that allowed us to measure the applied load, which we found was proportional to pressure during calibration runs (26). We estimated pressure between 335 GPa and 495 GPa using this calibration. We increased the load (pressure) by rotating a screw with a long stainless steel tube attached to the DAC in the cryostat. Increasing the pressure by rotating the screw after the 335 GPa pressure point resulted in our sample starting to turn black (Fig. 2B) as it transitioned into the  $H_2$ -PRE phase (24). Earlier studies of hydrogen reported the sample as black at lower pressures (28), but we believe that this is a result of different pressure calibrations in this high pressure region (26).

After some more screw turns (fig. S3) the sample reflectance changed from black to high reflectivity, characteristic of a metal (Fig. 2C). We then studied the wavelength dependence of the reflectance of the sample at liquid nitrogen and liquid helium temperatures (Fig. 3). In order to do this

the stereo microscope, used for visual observation (Fig. 2), was replaced with a high-resolution long working-distance microscope (Wild Model 420 Macroscope) that not only allowed visual observation, but also allowed an attenuated laser beam to be co-focused with the microscope image. In order to measure the reflectance we wanted to magnify the image of the sample and project it on a camera. The Macroscopic (fig. S5) (26) enables an external image to be formed that can be further magnified for a total calibrated magnification of  $\sim 44$ ; this was imaged onto a color CMOS camera (Thorlabs DC1645C). We can select the area of interest (effectively spatial filtering) and measure the reflectance from different surfaces (fig. S6). We measured the reflectance from the metallic hydrogen and the rhenium gasket. We measured at three wavelengths in the visible spectral region, using both broadband white light, and three narrow band lasers that illuminated the sample (26), as well as one wavelength in the infrared. The measured reflectances are shown in Fig. 3, along with measurements of reflectance of the Re gasket, and reflectance from a sheet of Re at ambient conditions, that agreed well with values from the literature (29).

At high pressure the stressed culet of the diamond becomes absorptive due to closing down of the diamond band gap (5.5 eV at ambient) (30). This attenuated both the incident and reflected light and is strongest in the blue. Fortunately this has been studied in detail by Vohra (31) who provided the optical density for both type I and II diamonds to very high pressures. We used this study (fig. S4) and determined the corrected reflectance (Fig. 3A). Finally, after we measured the reflectance, we used very low laser power (642.6 nm laser wavelength) and measured the Raman shift of the diamond phonon to be  $2034\text{ cm}^{-1}$ . This value fixes the end-point of our rotation or load scale, as the shift of the diamond phonon line has been calibrated. The linear 2006 scale of Akahama and Kawamura (32) gives a pressure of  $495 \pm 13$  GPa when the sample was metallic. We do not include the potentially large systematic uncertainty in the pressure (26). This is the highest pressure point on our pressure vs. load or rotation scale (fig. S3). Such curves eventually saturate, i.e., the pressure does not increase as the load is increased.

An analysis of the reflectance can yield important information concerning the fundamental properties of a metal. A very successful and easy to implement model is the Drude free electron model of a metal (33). This model of a metal is likely a good approximation to relate reflectance to fundamental properties of a metal. A recent band structure analysis of the  $I4_1/amd$  space group by Borinaga *et al.* (9) shows that for this structure, electrons in SMH are close to the free-electron limit, which supports the application of a Drude model. The Drude model has two parameters, the plasma frequency  $\omega_p$ , and the relaxation time  $\tau$ . The plasma

frequency is given by  $\omega_p^2 = 4\pi n_e^2 / m_e$  where  $m_e$  and  $e$  are the electron mass and charge, and  $n_e$  is the electron density. The complex index of refraction of metallic hydrogen is given by  $N_H^2 = 1 - \omega_p^2 / (\omega^2 + j\omega/\tau)$ , where  $\omega$  is the angular frequency of the light. The metallic hydrogen is in contact with the stressed diamond that has an index of refraction  $N_D$ ; this has a value of  $\sim 2.41$  in the red region of the spectrum at ambient conditions. We measured reflectance  $R(\omega) = |(N_D - N_H)/(N_D + N_H)|^2$  as a function of energy or (angular) frequency  $\omega$ . A least-squares fit to the corrected reflectance data was used to determine the Drude parameters; at 5 K  $32.5 \pm 2.1$  eV and  $6.7 \pm 0.6 \times 10^{16}$  sec. These values differ appreciably from a fit to the uncorrected data.

Because the diamond culet is stressed, we expect the index of refraction in the region of contact with the metallic hydrogen to change from the value at ambient pressure, and this might lead to an important uncertainty in the fitting parameters. The index of the diamond under pressure and uniaxial stress has been studied by Surh *et al.* (34). For hydrostatic pressures up to 450 GPa, the pressure dependence is rather weak; however, for uniaxial stressed diamond the change of index can be substantial. We fitted data for values of 2.12 and 2.45 for extreme uniaxial stress along the [001] crystal direction, and [100] and [010] directions, respectively, corresponding to a sample pressure of 250 GPa (34). This resulted in an uncertainty in the Drude parameters that was much smaller than that due to the uncertainty in the measured reflectance (Fig. 3). We fit the reflectance using a value  $N_D = 2.41$ , yielding the values for the Drude parameters shown in Fig. 3 and Table 1.

Figure 4 shows the pressure-temperature phase diagram of hydrogen along Pathway I, focusing on the lower temperature region. With increasing pressure, hydrogen enters the phase H<sub>2</sub>-PRE at 355 GPa and this is followed by the phase line based on the two points at  $T = 83$  and 5.5 K for the transition to metallic hydrogen. (24). Because we changed the pressure in larger increments by rotating a screw, there could be a systematic uncertainty of about 25 GPa on the low-pressure side of the phase line. The transition to metallic hydrogen may have taken place while increasing the pressure from about 465 to 495 GPa (26). We believe the metallic phase is most likely solid, based on recent theory (35), but we do not have experimental evidence to discriminate between the solid and liquid states. We detected no visual change in the sample when the temperature was varied between 83 and 5.5 K. A theoretical analysis predicted a maximum in the pressure-temperature melting line of hydrogen (36). The maximum was first experimentally observed by Deemyad and Silvera (37). One speculation has the melting line (Fig. 1) extrapolating to the  $T = 0$  K limit at

high pressure resulting in liquid metallic hydrogen in this limit (36), (10). An extrapolation of the negative P,T slope was supported by a calculation (38) showing that the liquid atomic phase might be the ground state in the low temperature limit. On the other hand, Zha (39) has extended the melting line to 300 GPa and finds a slope that is shallower than the extrapolation shown in Fig. 1. The vibron spectra at low temperature in phase H<sub>2</sub>-PRE correspond to spectra from a solid. Although H<sub>2</sub>-PRE is solid, the possibility remains that an increase in translational zero-point energy occurs when molecular hydrogen dissociates resulting in a liquid ground state.

The plasma frequency  $\omega_p = 32.5 \pm 2.1$  eV is related to the electron density and yields a value of  $n_e = 7.7 \pm 1.1 \times 10^{23}$  particles/cm<sup>3</sup>. No experimental measurements exist for the atom density at 500 GPa. Theoretical estimates range from  $\sim 6.6$  to  $8.8 \times 10^{23}$  particles/cm<sup>3</sup> (26). This is consistent with one electron per atom, so molecular hydrogen is dissociated and the sample is atomic metallic hydrogen, or the WH phase. While some predictions suggest metallization of molecular hydrogen at high pressure (39), this requires one electron for every two atoms instead. Metallic hydrogen at 495 GPa is about 15-fold denser than zero-pressure molecular hydrogen. We compared metallic hydrogen to other elements in the first column of the periodic table (Table 1), which has a remarkable contrast in properties.

We have produced atomic metallic hydrogen in the laboratory at high pressure and low temperature. Metallic hydrogen may have important impact on physics and perhaps will ultimately find wide technological application. Theoretical work suggests a wide array of interesting properties for metallic hydrogen, including high temperature superconductivity and superfluidity (if a liquid) (40). A looming challenge is to quench metallic hydrogen and if so study its temperature stability to see if there is a pathway for production in large quantities.

## REFERENCES AND NOTES

1. V. L. Ginzburg, Nobel Lecture: On superconductivity and superfluidity (what I have and have not managed to do) as well as on the "physical minimum" at the beginning of the XXI century. *Rev. Mod. Phys.* **76**, 981–998 (2004). [doi:10.1103/RevModPhys.76.981](https://doi.org/10.1103/RevModPhys.76.981)
2. E. Wigner, H. B. Huntington, On the possibility of a metallic modification of hydrogen. *J. Chem. Phys.* **3**, 764–770 (1935). [doi:10.1063/1.1749590](https://doi.org/10.1063/1.1749590)
3. J. M. McMahon, M. A. Morales, C. Pierleoni, D. M. Ceperley, The properties of hydrogen and helium under extreme conditions. *Rev. Mod. Phys.* **84**, 1607–1653 (2012). [doi:10.1103/RevModPhys.84.1607](https://doi.org/10.1103/RevModPhys.84.1607)
4. J. McMinis, R. C. Clay, D. Lee, M. A. Morales, Molecular to atomic phase transition in hydrogen under high pressure. *Phys. Rev. Lett.* **114**, 105305 (2015). [doi:10.1103/PhysRevLett.114.105305](https://doi.org/10.1103/PhysRevLett.114.105305) [Medline](#)
5. S. Azadi, B. Monserrat, W. M. C. Foulkes, R. J. Needs, Dissociation of high-pressure solid molecular hydrogen: A quantum Monte Carlo and anharmonic vibrational study. *Phys. Rev. Lett.* **112**, 165501 (2014). [doi:10.1103/PhysRevLett.112.165501](https://doi.org/10.1103/PhysRevLett.112.165501) [Medline](#)
6. J. M. McMahon, D. M. Ceperley, Ground-state structures of atomic metallic hydrogen. *Phys. Rev. Lett.* **106**, 165302–165304 (2011). [doi:10.1103/PhysRevLett.106.165302](https://doi.org/10.1103/PhysRevLett.106.165302) [Medline](#)



7. N. W. Ashcroft, Metallic Hydrogen: A High Temperature Superconductor? *Phys. Rev. Lett.* **21**, 1748–1749 (1968). [doi:10.1103/PhysRevLett.21.1748](https://doi.org/10.1103/PhysRevLett.21.1748)
8. J. M. McMahon, D. M. Ceperley, High-temperature superconductivity in atomic metallic hydrogen. *Phys. Rev. B* **84**, 144515 (2011). [doi:10.1103/PhysRevB.84.144515](https://doi.org/10.1103/PhysRevB.84.144515)
9. M. Borinaga, I. Errea, M. Calandra, F. Mauri, A. Bergara, Anharmonic effects in atomic hydrogen: Superconductivity and lattice dynamical stability. *Phys. Rev. B* **93**, 174308 (2016). [doi:10.1103/PhysRevB.93.174308](https://doi.org/10.1103/PhysRevB.93.174308)
10. E. G. Brovman, Y. Kagan, A. Kholas, Structure of Metallic Hydrogen at Zero Pressure. *Sov. Phys. JETP* **34**, 1300–1315 (1972).
11. J. Cole, I. F. Silvera, J. P. Foote, in *STAIF-2008*, A. C. P. 978, Ed. (Albuquerque, NM, 2008), vol. AIP Conf. Proc 978, pp. 977–984.
12. M. Zaghoo, A. Salamat, I. F. Silvera, Evidence of a first-order phase transition to metallic hydrogen. *Phys. Rev. B* **93**, 155128 (2016). [doi:10.1103/PhysRevB.93.155128](https://doi.org/10.1103/PhysRevB.93.155128)
13. S. T. Weir, A. C. Mitchell, W. J. Nellis, Metallization of fluid molecular hydrogen at 140 GPa (1.4 Mbar). *Phys. Rev. Lett.* **76**, 1860–1863 (1996). [doi:10.1103/PhysRevLett.76.1860](https://doi.org/10.1103/PhysRevLett.76.1860) [Medline](#)
14. V. E. Fortov, R. I. Ilkaev, V. A. Arin, V. V. Burtzev, V. A. Golubev, I. L. Iosilevskiy, V. V. Khrustalev, A. L. Mikhailov, M. A. Mochalov, V. Y. Ternovoi, M. V. Zhernokletov, Phase transition in a strongly nonideal deuterium plasma generated by quasi-isentropic compression at megabar pressures. *Phys. Rev. Lett.* **99**, 185001–185004 (2007). [doi:10.1103/PhysRevLett.99.185001](https://doi.org/10.1103/PhysRevLett.99.185001) [Medline](#)
15. M. D. Knudson, M. P. Desjarlais, A. Becker, R. W. Lemke, K. R. Cochrane, M. E. Savage, D. E. Bliss, T. R. Mattsson, R. Redmer, Direct observation of an abrupt insulator-to-metal transition in dense liquid deuterium. *Science* **348**, 1455–1460 (2015). [doi:10.1126/science.aaa7471](https://doi.org/10.1126/science.aaa7471) [Medline](#)
16. C. Pierleoni, M. A. Morales, G. Rillo, M. Holzmann, D. M. Ceperley, Liquid-liquid phase transition in hydrogen by coupled electron-ion Monte Carlo simulations. *Proc. Natl. Acad. Sci. U.S.A.* **113**, 4953–4957 (2016). [doi:10.1073/pnas.1603853113](https://doi.org/10.1073/pnas.1603853113) [Medline](#)
17. G. E. Norman, I. M. Saitov, V. V. Stegailov, Plasma-Plasma and Liquid-liquid first-order phase transitions. *Plasma Phys.* **55**, 215–221 (2015). [doi:10.1002/ctpp.201400088](https://doi.org/10.1002/ctpp.201400088)
18. I. F. Silvera, The Solid Molecular Hydrogens in the Condensed Phase: Fundamentals and Static Properties. *Rev. Mod. Phys.* **52**, 393–452 (1980). [doi:10.1103/RevModPhys.52.393](https://doi.org/10.1103/RevModPhys.52.393)
19. I. F. Silvera, R. J. Wijngaarden, New Low Temperature Phase of Molecular Deuterium at Ultra High Pressure. *Phys. Rev. Lett.* **47**, 39–42 (1981). [doi:10.1103/PhysRevLett.47.39](https://doi.org/10.1103/PhysRevLett.47.39)
20. R. J. Hemley, H. K. Mao, Phase transition in solid molecular hydrogen at ultrahigh pressures. *Phys. Rev. Lett.* **61**, 857–860 (1988). [doi:10.1103/PhysRevLett.61.857](https://doi.org/10.1103/PhysRevLett.61.857) [Medline](#)
21. H. E. Lorenzana, I. F. Silvera, K. A. Goettel, Evidence for a structural phase transition in solid hydrogen at megabar pressures. *Phys. Rev. Lett.* **63**, 2080–2083 (1989). [doi:10.1103/PhysRevLett.63.2080](https://doi.org/10.1103/PhysRevLett.63.2080) [Medline](#)
22. M. I. Eremets, I. A. Troyan, Conductive dense hydrogen. *Nat. Mater.* **10**, 927–931 (2011). [doi:10.1038/nmat3175](https://doi.org/10.1038/nmat3175) [Medline](#)
23. R. T. Howie, C. L. Guillaume, T. Scheler, A. F. Goncharov, E. Gregoryanz, Mixed molecular and atomic phase of dense hydrogen. *Phys. Rev. Lett.* **108**, 125501 (2012). [doi:10.1103/PhysRevLett.108.125501](https://doi.org/10.1103/PhysRevLett.108.125501) [Medline](#)
24. R. Dias, O. Noked, I. F. Silvera, New Quantum Phase Transition in Dense Hydrogen: The Phase Diagram to 420 GPa. *arXiv:1603.02162v1*, (2016).
25. M. I. Eremets, I. A. Troyan, A. P. Drozdov, Low temperature phase diagram of hydrogen at pressures up to 380 GPa. A possible metallic phase at 360 GPa and 200 K. *arXiv:1601.04479*, (2016).
26. Materials and Methods are available as supplementary materials.
27. M. I. Eremets, Megabar high pressure cells for Raman measurements. *J. Raman Spectrosc.* **34**, 515–518 (2003). [doi:10.1002/jrs.1044](https://doi.org/10.1002/jrs.1044)
28. P. Loubeyre, F. Occelli, R. LeToullec, Optical studies of solid hydrogen to 320 GPa and evidence for black hydrogen. *Nature* **416**, 613–617 (2002). [doi:10.1038/416613a](https://doi.org/10.1038/416613a) [Medline](#)
29. E. D. Palik, Ed., *Handbook of Optical Constants of Solids*, (1997), vol. III.
30. A. L. Ruoff, H. Luo, Y. K. Vohra, The closing diamond anvil optical window in multimegabar research. *J. Appl. Phys.* **69**, 6413–6416 (1991). [doi:10.1063/1.348845](https://doi.org/10.1063/1.348845)
31. Y. K. Vohra, in *Proceedings of the XIII AIRAPT International Conference on High Pressure Science and Technology*. (1991, Bangalore, India, 1991).
32. Y. Akahama, H. Kawamura, Pressure calibration of diamond anvil Raman gauge to 310 GPa. *J. Appl. Phys.* **100**, 043516 (2006). [doi:10.1063/1.2335683](https://doi.org/10.1063/1.2335683)
33. F. Wooten, *Optical Properties of Solids*. (Academic Press, New York, 1972), pp. 260.
34. M. P. Surh, S. G. Louie, M. L. Cohen, Band gaps of diamond under anisotropic stress. *Phys. Rev. B Condens. Matter* **45**, 8239–8247 (1992). [doi:10.1103/PhysRevB.45.8239](https://doi.org/10.1103/PhysRevB.45.8239) [Medline](#)
35. J. Chen, X.-Z. Li, Q. Zhang, M. I. J. Probert, C. J. Pickard, R. J. Needs, A. Michaelides, E. Wang, Quantum simulation of low-temperature metallic liquid hydrogen. *Nat. Commun.* **4**, 2064 (2013). [doi:10.1038/ncomms3064](https://doi.org/10.1038/ncomms3064) [Medline](#)
36. S. A. Bonev, E. Schwegler, T. Ogitsu, G. Galli, A quantum fluid of metallic hydrogen suggested by first-principles calculations. *Nature* **431**, 669–672 (2004). [doi:10.1038/nature02968](https://doi.org/10.1038/nature02968) [Medline](#)
37. S. Deemyad, I. F. Silvera, Melting line of hydrogen at high pressures. *Phys. Rev. Lett.* **100**, 155701 (2008). [doi:10.1103/PhysRevLett.100.155701](https://doi.org/10.1103/PhysRevLett.100.155701) [Medline](#)
38. C. Attaccalite, S. Sorella, Stable liquid hydrogen at high pressure by a novel *Ab initio* molecular-dynamics calculation. *Phys. Rev. Lett.* **100**, 114501 (2008). [doi:10.1103/PhysRevLett.100.114501](https://doi.org/10.1103/PhysRevLett.100.114501) [Medline](#)
39. C. S. Zha, in *Bull. Am. Phys. Soc.* (APS, Baltimore, MD, 2016).
40. E. Babaev, A. Sudbø, N. W. Ashcroft, A superconductor to superfluid phase transition in liquid metallic hydrogen. *Nature* **431**, 666–668 (2004). [doi:10.1038/nature02910](https://doi.org/10.1038/nature02910) [Medline](#)
41. I. F. Silvera, R. J. Wijngaarden, Diamond Anvil Cell and Cryostat for Low Temperature Optical Studies. *Rev. Sci. Instrum.* **56**, 121–124 (1985). [doi:10.1063/1.1138514](https://doi.org/10.1063/1.1138514)
42. N. H. Chen, I. F. Silvera, Excitation of Ruby Fluorescence at Multimegabar Pressures. *Rev. Sci. Instrum.* **67**, 4275–4278 (1996). [doi:10.1063/1.1147526](https://doi.org/10.1063/1.1147526)
43. A. Chijioke, W. J. Nellis, A. Soldatov, I. F. Silvera, The Ruby Pressure Standard to 150 GPa. *J. Appl. Phys.* **98**, 114905 (2005). [doi:10.1063/1.2135877](https://doi.org/10.1063/1.2135877)
44. H. K. Mao, J. Xu, P. M. Bell, Calibration of the Ruby Pressure Gauge to 800 kbar Under Quasi-Hydrostatic Conditions. *J. Geophys. Res.* **91** (B5), 4673–4676 (1986). [doi:10.1029/JB091iB05p04673](https://doi.org/10.1029/JB091iB05p04673)
45. C. Narayana, H. Luo, J. Orloff, A. L. Ruoff, Solid hydrogen at 342 GPa: No evidence for an alkali metal. *Nature* **393**, 46–49 (1998). [doi:10.1038/29949](https://doi.org/10.1038/29949)
46. I. F. Silvera, in *AIRAPT*. (Forschungszentrum Karlsruhe [http://bibliothek.fzk.de/zb/verlagspublikationen/AIRAPT\\_EHPRG2005/](http://bibliothek.fzk.de/zb/verlagspublikationen/AIRAPT_EHPRG2005/), Karlsruhe, Germany, 2005), vol. plenaries.
47. C.-S. Zha, Z. Liu, R. J. Hemley, Synchrotron infrared measurements of dense hydrogen to 360 GPa. *Phys. Rev. Lett.* **108**, 146402–146407 (2012). [doi:10.1103/PhysRevLett.108.146402](https://doi.org/10.1103/PhysRevLett.108.146402) [Medline](#)
48. M. Hanfland, K. Syassen, A Raman Study of Diamond Anvils under Stress. *J. Appl. Phys.* **57**, 2752–2756 (1985). [doi:10.1063/1.335417](https://doi.org/10.1063/1.335417)
49. H. Boppart, J. van Straaten, I. F. Silvera, Raman spectra of diamond at high pressures. *Phys. Rev. B Condens. Matter* **32**, 1423–1425 (1985). [doi:10.1103/PhysRevB.32.1423](https://doi.org/10.1103/PhysRevB.32.1423) [Medline](#)
50. Y. Akahama, H. Kawamura, Diamond anvil Raman gauge in multimegabar pressure range. *High Press. Res.* **27**, 473–482 (2007). [doi:10.1080/08957950701659544](https://doi.org/10.1080/08957950701659544)
51. Y. Akahama, H. Kawamura, Pressure calibration of diamond anvil Raman gauge to 410 GPa. *J. Phys. Conf. Ser.* **215**, 012195 (2010). [doi:10.1088/1742-6596/215/1/012195](https://doi.org/10.1088/1742-6596/215/1/012195)
52. B. J. Baer, M. E. Chang, W. J. Evans, Raman shift of stressed diamond anvils: Pressure calibration and culet geometry dependence. *J. Appl. Phys.* **104**, 034504 (2008). [doi:10.1063/1.2963360](https://doi.org/10.1063/1.2963360)
53. R. T. Howie, E. Gregoryanz, A. F. Goncharov, Hydrogen (deuterium) vibron frequency as a pressure comparison gauge at multi-Mbar pressures. *J. Appl. Phys.* **114**, 073505–073506 (2013). [doi:10.1063/1.4818606](https://doi.org/10.1063/1.4818606)
54. Y. K. Vohra, in *AIRAPT: Recent Trends in High Pressure Research*, A. K. Singh, Ed. (Oxford Press, New Delhi, India, 1992, Bangalore, India, 1991), vol. Proceedings of the XIII AIRAPT International Conference, pp. 349–358.
55. P. Loubeyre, R. LeToullec, D. Hausermann, M. Hanfland, R. J. Hemley, H. K. Mao, L. W. Finger, X-ray Diffraction and Equation of State of Hydrogen at Megabar

- Pressures. *Nature* **383**, 702–704 (1996). doi:10.1038/383702a0
56. N. W. Ashcroft, Hydrogen at high density. *J. Phys. A* **36**, 6137–6147 (2003). doi:10.1088/0305-4470/36/22/341
  57. G. W. Collins, P. Celliers, D. M. Gold, M. E. Foord, R. J. Wallace, A. Ng, S. V. Weber, K. S. Budil, R. Cauble, Da Silva LB, Measurements of the equation of state of deuterium at the fluid insulator-metal transition. *Science* **281**, 1178–1181 (1998). doi:10.1126/science.281.5380.1178 Medline
  58. P. M. Celliers, G. W. Collins, L. B. Da Silva, D. M. Gold, R. Cauble, R. J. Wallace, M. E. Foord, B. A. Hammel, Shock-induced transformation of liquid deuterium into a metallic fluid. *Phys. Rev. Lett.* **84**, 5564–5567 (2000). doi:10.1103/PhysRevLett.84.5564 Medline
  59. G. W. Collins, P. M. Celliers, L. B. Da Silva, R. Cauble, D. M. Gold, M. E. Foord, N. C. Holmes, B. A. Hammel, R. J. Wallace, A. Ng, Temperature measurements of shock compressed liquid deuterium up to 230 GPa. *Phys. Rev. Lett.* **87**, 165504 (2001). doi:10.1103/PhysRevLett.87.165504 Medline
  60. P. Loubeyre, S. Brygoo, J. Eggert, P. M. Celliers, D. K. Spaulding, J. R. Rygg, T. R. Boehly, G. W. Collins, R. Jeanloz, Extended data set for the equation of state of warm dense hydrogen isotopes. *Phys. Rev. B* **86**, 144115 (2012). doi:10.1103/PhysRevB.86.144115

## ACKNOWLEDGMENTS

We thank Ori Noked, Mohamed Zaghoo, Rachel Husband, and Chad Meyers for assistance and discussions. Ori Noked provided valuable assistance developing our general optical setup, Rachel Husband did the reactive ion etching, as well as the alumina coating of the diamonds, and Mathew Turner of the Walsworth group provided help for annealing our diamonds. The NSF, grant DMR-1308641 and the DoE Stockpile Stewardship Academic Alliance Program, grant DE-NA0003346, supported this research. Partial support was provided by a grant from Alby and Kim Silvera. Preparation of diamond surfaces was performed in part at the Center for Nanoscale Systems (CNS), a member of the National Nanotechnology Infrastructure Network (NNIN), which is supported by the National Science Foundation under NSF award no. ECS-0335765. CNS is part of Harvard University. The data reported in this paper are tabulated and available from the authors. Both authors contributed equally to all aspects of this research.

## SUPPLEMENTARY MATERIALS

[www.sciencemag.org/cgi/content/full/science.aal1579/DC1](http://www.sciencemag.org/cgi/content/full/science.aal1579/DC1)

Materials and Methods

Figs. S1 to S8

Databases S1 to S14

References (43–60)

5 October 2016; accepted 13 January 2017

Published online 26 January 2017

10.1126/science.aal1579

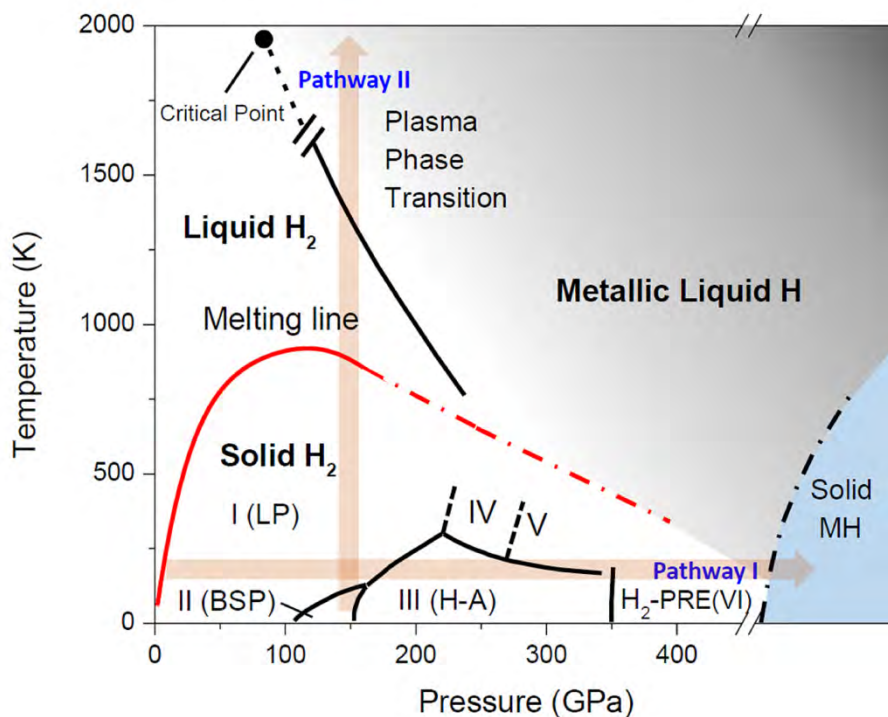


**Fig. 1. Experimental/theoretical P-T phase diagram of hydrogen.** Shown are two pathways to metallic hydrogen, I the low temperature pathway and II the high temperature pathway. In pathway I phases for pure para hydrogen have lettered names: LP (low pressure), BSP (broken symmetry phase) and H-A (hydrogen-A). The plasma phase transition (PPT) is the transition to liquid metallic atomic hydrogen.

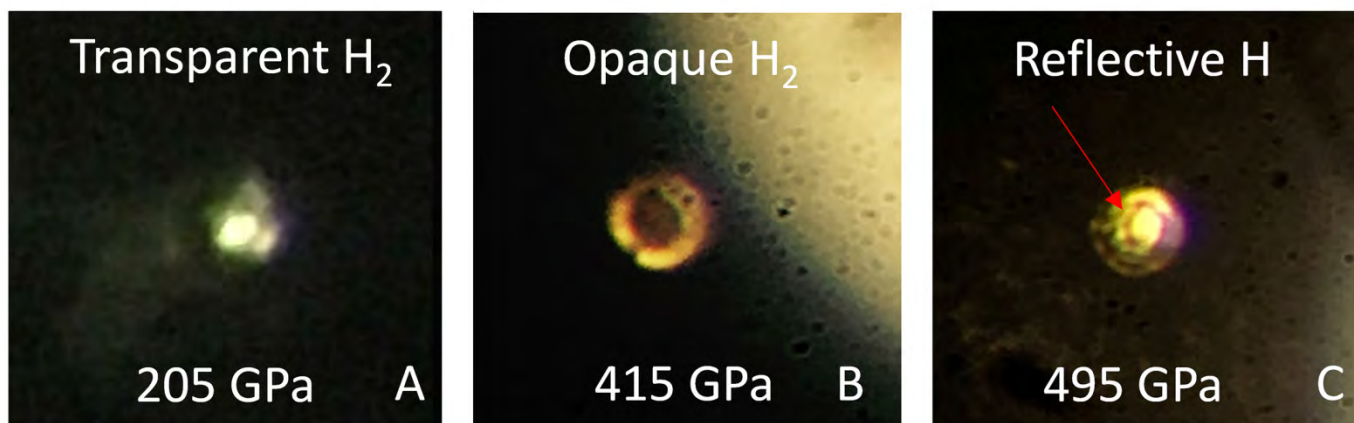


**Fig. 2. Photographs of hydrogen at different stages of compression.** Photos were taken with an iphone camera at the ocular of a modified stereo microscope, using LED illumination in the other optical path of the microscope. (A) At pressures to 335 GPa hydrogen was transparent. The sample was both front and back illuminated in this and in B; the less bright area around the sample is light reflected off of the Re gasket. (B) At this stage of compression the sample was black and non-transmitting. The brighter area to the upper right corner is due to the LED illumination which was not focused on the sample for improved contrast; (C) Photo of metallic hydrogen at a pressure of 495 GPa. The sample is non-transmitting and is observed in reflected light. The central region is clearly more reflective than the surrounding metallic rhenium gasket. The sample dimensions are approximately 8-10 microns with thickness ~1.2 microns (27).

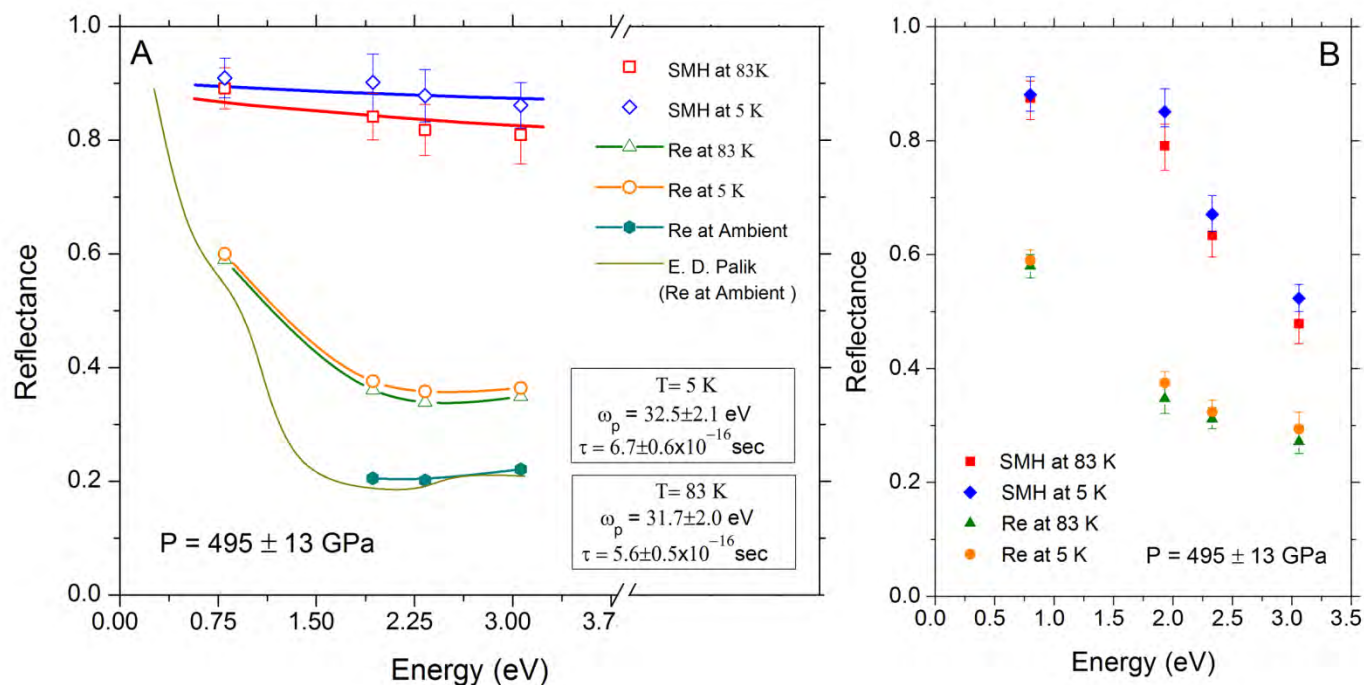


**Fig. 3. Reflectance as a function of photon energy.** (A) The energy dependence of the normal incidence reflectance off metallic hydrogen and the rhenium gasket,  $P = 495$  GPa, at liquid nitrogen and liquid helium temperatures. We also show our measured reflectance from a surface of Re at a pressure of 1 bar at room temperature; this is in good agreement with literature values, verifying our measurement procedure. The reflectances have been corrected for absorption in the diamond. The lines through MH data are fits with a Drude free electron model; the lines through the Re data points are guides to the eye. (B) Raw reflectance data without the diamond absorption correction. The uncertainties in the data points are from measurement of the reflectance and the correction procedure and represent random errors.



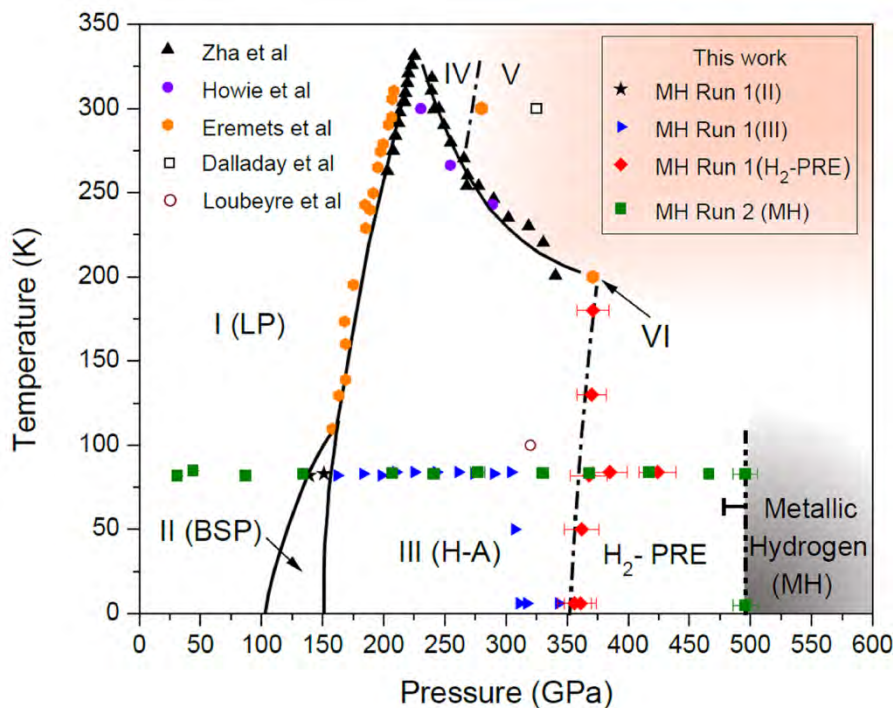


**Fig. 4. The T-P phase diagram of hydrogen along Pathway I of Fig. 1.** The data shows the thermodynamic pathway followed for our measurements. We also show other recent data for the phases at lower pressures from Zha *et al.* (40), Howie *et al.*, Eremets *et al.* (25), and Dias *et al.* (24). A transition claimed by Dalladay-Simpson *et al.* (41) at 325 GPa is plotted as a point, as is the earlier observation of black hydrogen by Loubeyre *et al.* (28).



**Table 1. Elements of the first column of the periodic table.** We compare the electron density (calculated from the plasma frequency) in the second column to the atom density in the third column, and see that there is about 1 electron/atom. The plasma frequencies are from Ref. (42). The data are for hydrogen at 5.5 K; all other elements are at 77 K. See ref. (27) for a definition of  $r_s/a_0$ .

Element	$n_e = \frac{m_e \omega_p^2}{4\pi e^2}$ ( $10^{22}/\text{cm}^3$ )	$n_a$ ( $10^{22}/\text{cm}^3$ )	$r_s/a_0$	Plasma frequency (eV)
H	$77 \pm 11$	66.5–86.0	1.255–1.34	$32.5 \pm 2.1$
Li	3.68	4.63	3.25	7.12
Na	2.36	2.54	3.93	5.71
K	1.00	1.33	4.86	3.72